Applied Surface Science 274 (2013) 328–333

Contents lists available at SciVerse ScienceDirect

Applied Surface Science

journal homepage: www.elsevier.com/locate/apsusc

Preparation of Cu-loaded $SrTiO_3$ nanoparticles and their photocatalytic activity for hydrogen evolution from methanol aqueous solution

Duc-Nguyen Bui[a,b], Jin Mu[a,*], Lei Wang[b], Shi-Zhao Kang[a], Xiangqing Li[a]

[a] School of Chemical and Environmental Engineering, Shanghai Institute of Technology, 100 Haiquan Road, Shanghai 201418, China
[b] School of Chemistry and Molecular Engineering, East China University of Science and Technology, 130 Meilong Road, Shanghai 200237, China

ARTICLE INFO

Article history:
Received 11 December 2012
Received in revised form 26 February 2013
Accepted 11 March 2013
Available online 16 March 2013

Keywords:
Cu co-catalyst
$SrTiO_3$ nanoparticles
Photocatalysis
Hydrogen

ABSTRACT

Cu-loaded $SrTiO_3$ nanoparticles (Cu–$SrTiO_3$) were prepared using a simple in situ photo-deposition method and their photocatalytic activity for hydrogen evolution from methanol aqueous solution was evaluated. The results characterized with XRD, TEM, XPS and EDX indicated that the as-synthesized sample was composed of metallic Cu and cubic $SrTiO_3$, and the metallic Cu was homogeneously loaded on the surface of $SrTiO_3$ nanoparticles. Under UV light irradiation, Cu–$SrTiO_3$ displayed much higher photocatalytic activity for hydrogen evolution and excellent stability in comparison with pure $SrTiO_3$ nanoparticles. The results further confirmed that the efficient separation of photogenerated electron/hole pairs was critical for the enhanced photocatalytic activity of Cu–$SrTiO_3$. Moreover, the rate of hydrogen evolution of 0.5 wt.% Cu–$SrTiO_3$ is comparable with that of 0.5 wt.% Pt–$SrTiO_3$ photocatalyst under optimum conditions, implying that the metallic Cu is an efficient alternative to Pt as a co-catalyst on $SrTiO_3$. The high photocatalytic activity, low cost and chemical stability mean that the Cu-loaded $SrTiO_3$ is a potential catalyst for the photocatalytic hydrogen evolution from methanol aqueous solution.

1. Introduction

Photocatalytic hydrogen evolution from water splitting has received much attention in recent years due to its potential application in providing hydrogen as a clean and renewable energy resource even on a large scale [1–4]. To enhance the efficiency of hydrogen evolution, considerable effort has been exerted to find an efficient photocatalyst. Important points in these photocatalysts are the width of band gap (E_g) and the levels of conduction and valence bands, which strongly determine whether a water-splitting reaction occurs or not [5–7]. As one of the most promising photocatalysts, perovskite-type $SrTiO_3$ has been widely studied to produce hydrogen by splitting water in which its band structure suits the water redox potential levels to facilitate the formation of hydrogen and oxygen [8–11]. However, the photocatalytic efficiency of pure $SrTiO_3$ for hydrogen evolution is very low due to the fast recombination of photogenerated electrons and holes, which hampers the extensive application of $SrTiO_3$ in photocatalysis.

There are two basic strategies to improve the efficiency of photosplitting water over $SrTiO_3$. The first one is that the addition of sacrificial reagents such as alcohols or other organic compounds could increase the rate of hydrogen evolution. The results described by Yi et al. show that methanol is one of the best capture reagents for the photogenerated holes of TiO_2 photocatalyst [12]. The second one is to load a metal or metal oxide co-catalyst onto the surface of $SrTiO_3$, which increases the charge transfer, reduces the recombination rate of photogenerated electrons and holes, and acts as an active site for hydrogen evolution [13–19]. It is reported that the photocatalytic activity of La-doped $SrTiO_3$ could be enhanced when NiO or CoO is used as a co-catalyst [20].

Compared with metal oxide co-catalysts, metals, especially noble metals such as Pt and Au, could more efficiently reduce the recombination of photo-generated electrons and holes due to the high Schottky barrier between the metal co-catalyst and the semiconductor photocatalyst. Thus, the metal co-catalyst may be more desirable than the metal oxide co-catalyst for practical applications. Additionally, the metal co-catalyst could be easily loaded on the surface of $SrTiO_3$ by a simple and mild reaction [21,22]. Because the noble metals, such as Pt and Au, are expensive and rare, it is worthwhile to find a Pt-free and low cost metal co-catalyst. It is known that the addition of Cu could significantly promote the photocatalytic hydrogen evolution of TiO_2 under UV light irradiation [23–25]. The Cu-loaded mesoporous TiO_2 photocatalyst shows two fold higher hydrogen evolution activity than the Ni-loaded one [26]. Moreover, oxidizing of metallic copper could enhance the hydrogen evolution activity of TiO_2 [27]. Accordingly, it is inferred that

* Corresponding author. Tel.: +86 21 60873061; fax: +86 21 60873567.
E-mail address: mujin@sit.edu.cn (J. Mu).

0169-4332/$ – see front matter © 2013 Elsevier B.V. All rights reserved.
http://dx.doi.org/10.1016/j.apsusc.2013.03.054

Cu could also be an efficient co-catalyst of $SrTiO_3$ for photocatalytic hydrogen evolution because the band-gap of $SrTiO_3$ is close to that of TiO_2. This paper aims to prove this inference. The Cu co-catalyst is loaded on the $SrTiO_3$ nanoparticles by using an in situ photo-deposition method. The photocatalytic activity of Cu–$SrTiO_3$ for hydrogen evolution is investigated using methanol as a sacrificial reagent. In addition, the reaction conditions including loading amount of Cu, reaction temperature, initial methanol concentration as well as dosage of photocatalyst are also discussed.

2. Experimental

2.1. Preparation of Cu-loaded $SrTiO_3$ nanoparticles

Strontium nitrate, citric acid and tetra-butyl titanate were used as starting materials for the synthesis of $SrTiO_3$. All materials were commercially available and used as received.

The $SrTiO_3$ nanoparticles were prepared by using a sol–gel method [28]. A typical experimental procedure was described as follows. A mixture of strontium nitrate (2.12 g) and citric acid (2.10 g) was added into deionized water (40 mL). Then, the pH value of the solution was adjusted to about 8 using aqueous ammonia. The solution obtained was denoted as solution **A**. An appropriate amount of tetra-butyl titanate (3.40 g) was dissolved into anhydrous ethanol (20 mL) under stirring, and the solution was denoted as solution **B**. Afterwards, solution **B** was slowly dropped into solution **A** under vigorous stirring. Then, the mixed solution obtained was vigorously stirred at 70 °C until it turned into a yellow glutinous sol. After the solvent was evaporated, the gel obtained was dried at 80 °C for 12 h to obtain a xerogel. Finally, the xerogel was calcined at 900 °C for 4 h with a heating rate of 5 °C/min, and then grinded to powder.

The $SrTiO_3$ nanoparticles loaded with various amounts of Cu (0.1, 0.25, 0.5, 1 and 1.5 wt.%) were prepared using a photo-deposition method. A typical experimental procedure of 0.5 wt.% Cu-loaded $SrTiO_3$ was described as follows. 120 mg of the as-prepared $SrTiO_3$ nanoparticles were dispersed into 60 mL of aqueous methanol solution (60 vol.%). Then, 0.95 mL of 0.01 M $Cu(NO_3)_2$ solution was added into the suspension. After bubbled with highly pure nitrogen (about 15 mL/min) for 30 min to remove the dissolved oxygen, the suspension was stirred and irradiated for 30 min by a 300 W high-pressure mercury lamp. The other Cu-loaded $SrTiO_3$ samples were prepared in similar procedures, and the obtained products are denoted as *x*% Cu–$SrTiO_3$ (*x* is the percentage of Cu loading).

For comparison, the Pt-loaded $SrTiO_3$ nanoparticles were prepared in a procedure similar to that of the Cu-loaded $SrTiO_3$ nanoparticles. Chloroplatinic acid ($H_2PtCl_6{\cdot}6H_2O$) was used as the Pt precursor.

2.2. Characterization

The powder X-ray diffraction (XRD) analysis was made on a Rigaku D/max 2550 VB/PC X-ray diffractometer (Japan) using Cu K1 radiation (wavelength = 0.154056 nm). The morphology of the samples was analyzed on a JEOL JEM-200CX transmission electron microscope (TEM) with 200 kV accelerating voltage (Japan). The X-ray photoelectron spectroscopy (XPS) was recorded with a PHI 5000 Versaprobe spectrometer (Japan). The diffuse reflectance ultraviolet–visible absorption spectra (DRS) were recorded on a Shimadzu UV-3101PC UV–vis–NIR spectrophotometer (Japan). The N_2 adsorption and desorption isotherms were measured on a Micromeritics ASAP-2020 nitrogen adsorption apparatus (USA). The photoluminescence spectra (PL) were recorded with a Shimadzu RF-5301PC fluorescence spectrometer (Japan). The energy-dispersive X-ray spectroscopy (EDX) was taken with a JEOL JSM-6360LV electron microscopy (Japan).

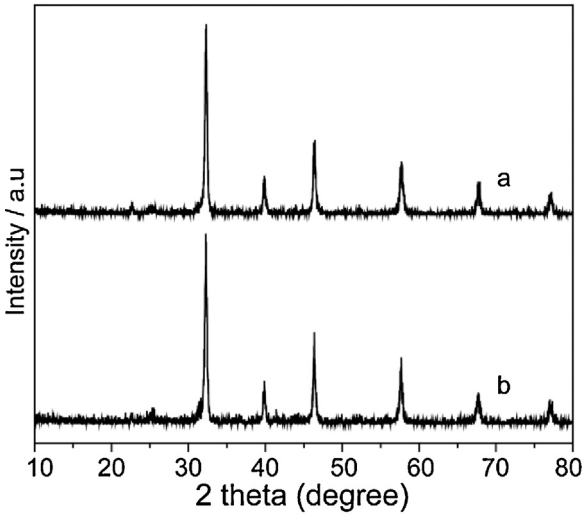

Fig. 1. XRD patterns of (a) pure $SrTiO_3$ and (b) 0.5% Cu–$SrTiO_3$.

2.3. Photocatalytic hydrogen evolution

The photocatalytic reaction was carried out in a gas-closed system with a quartz reactor. A 300 W high-pressure mercury lamp was used as UV light radiation source. In order to remove infrared light, the lamp was equipped with a water jacket. The distance between the lamp and the reactor was maintained to be 20 cm. The Cu–$SrTiO_3$ prepared by in situ photo-reduction was directly used in photocatalytic hydrogen evolution without further separation. The amount of hydrogen evolution was analyzed with a gas chromatograph (GC-112A, molecular sieve 5A, TCD, China) using nitrogen as carrier gas.

3. Results and discussion

3.1. Structure and composition of Cu–$SrTiO_3$

The XRD patterns of pure $SrTiO_3$ and 0.5% Cu–$SrTiO_3$ are shown in Fig. 1. It is clearly found that there exist six peaks at 32.4°, 39.9°, 46.4°, 57.8°, 67.8° and 77.2° in both of XRD patterns, corresponding to the (1 1 0), (1 1 1), (2 0 0), (2 1 1), (2 2 0) and (3 1 0) planes of cubic $SrTiO_3$ (JCPDS card no. 35-0734), respectively. Thus, the Cu–$SrTiO_3$ obtained possesses the cubic crystal phase. As shown in Fig. 1b, the diffraction peaks of Cu are not observed obviously in the XRD pattern of 0.5% Cu–$SrTiO_3$. A possible explanation is that the loading amount of Cu is few, or the Cu particles are too small to give well-defined diffraction peaks. Besides, the diffraction peaks of 0.5% Cu–$SrTiO_3$ do not shift in comparison with those of pure $SrTiO_3$. In situ photocatalytic reduction of Cu salt favors the formation of metallic Cu [25]. Therefore, it can be deduced that Cu atoms are not incorporated into the $SrTiO_3$ lattice [22].

The morphologies of pure $SrTiO_3$ and 0.5% Cu–$SrTiO_3$ were characterized with TEM. As shown in Fig. 2b, the introduction of Cu does not obviously change the morphology of $SrTiO_3$ nanoparticles compared with the TEM image of pure $SrTiO_3$ (Fig. 2a). The mean diameter of the Cu-loaded $SrTiO_3$ nanoparticles is approximately 30 nm, and their surfaces are fairly smooth. In addition, the composition of 0.5% Cu–$SrTiO_3$ was obtained by EDX analysis (not shown here) and XPS analysis (Fig. 3). The result of EDX shows that the product is composed of the elements Sr, Ti, O and Cu. The XPS analysis also confirmed that there exist elements Sr, Ti, O and

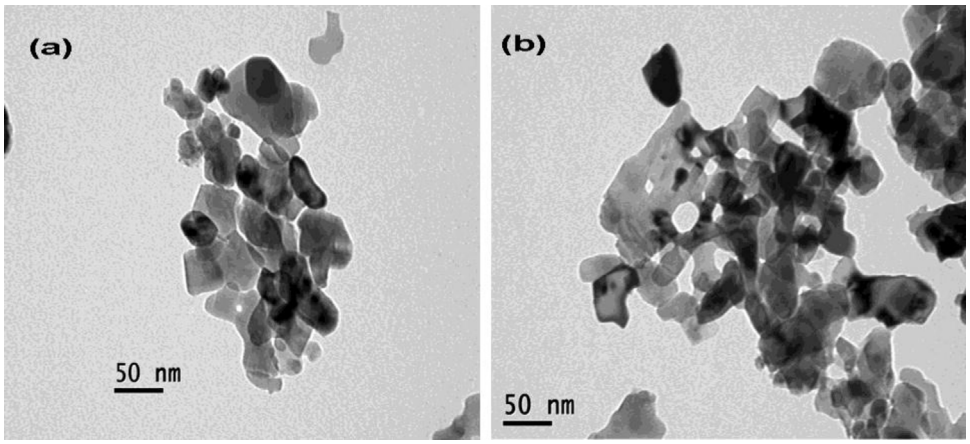

Fig. 2. TEM images of (a) pure $SrTiO_3$ and (b) 0.5% Cu–$SrTiO_3$.

Cu on the surface of 0.5% Cu–$SrTiO_3$ (Fig. 3A). Furthermore, high-resolution XPS of Cu 2p (Fig. 3B) shows that there exist two peaks at 932.62 eV and 952.5 eV, corresponding to Cu-$2p_{3/2}$ and Cu-$2p_{1/2}$ of metallic Cu, respectively, suggesting that metallic Cu is present on the surface of $SrTiO_3$ nanoparticles. Based on above results, the component of the as-synthesized sample could be defined as Cu and $SrTiO_3$. Moreover, when the EDX measurement was made on the various regions of the same sample, the amount of element Cu was constant within an error of ±5%, indicating that the metallic Cu was homogeneously loaded on the surface of $SrTiO_3$ nanoparticles.

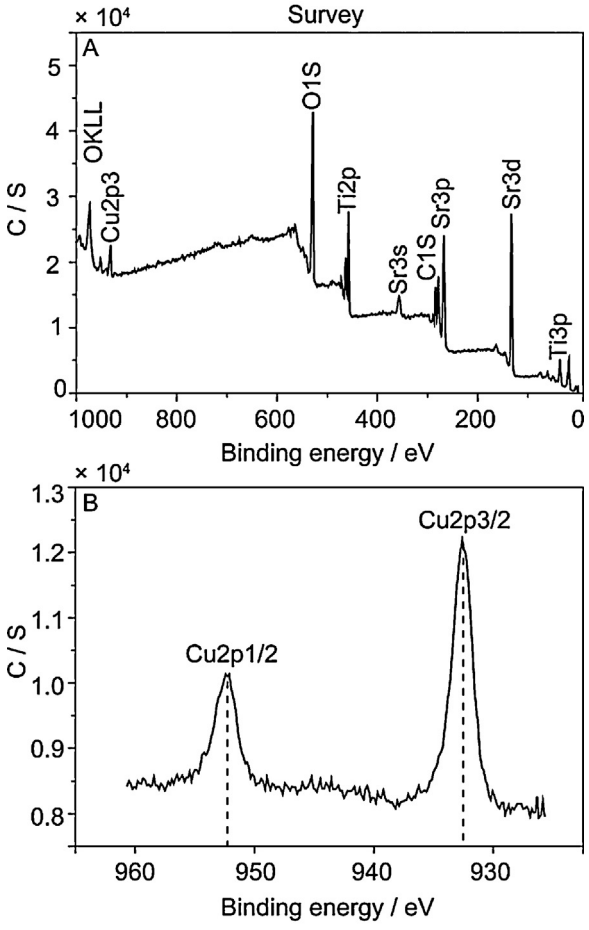

Fig. 3. (A) Survey XPS of 0.5% Cu–$SrTiO_3$ and (B) high-resolution XPS of Cu 2p.

3.2. Photocatalytic hydrogen evolution over 0.5% Cu–$SrTiO_3$

Fig. 4 displays the irradiation time courses of hydrogen evolution catalyzed by 0.5% Cu–$SrTiO_3$ and pure $SrTiO_3$. Under UV light irradiation for 48 h, the total amount of hydrogen evolution over 0.5% Cu–$SrTiO_3$ could be up to 14.3 mmol. Whereas, the total amount of hydrogen evolution over pure $SrTiO_3$ is only 0.08 mmol. Additionally, 0.5% Cu–$SrTiO_3$ could still keep highly photocatalytic activity after 48 h irradiation. These results indicate that Cu–$SrTiO_3$ is an efficient and stable photocatalyst under UV light irradiation.

The Brunauer–Emmett–Teller (BET) measurement shows that the specific surface areas of 0.5% Cu–$SrTiO_3$ and pure $SrTiO_3$ are 12.3 and 16.2 $m^2\,g^{-1}$, respectively. Also, the morphology of 0.5% Cu–$SrTiO_3$ is similar to that of pure $SrTiO_3$ (Fig. 2). Based on these results, the enhanced photocatalytic activity of 0.5% Cu–$SrTiO_3$ ought to be ascribed to the efficient separation of photogenerated electron/hole pairs.

For comparison, the photocatalytic hydrogen evolution over the Pt–$SrTiO_3$ nanoparticles was measured under the identical conditions. As can be seen from Table 1, after irradiation for 2 h, the maximum amount of hydrogen evolution (1065 μmol) is obtained over 2.0% Pt–$SrTiO_3$, and the amount of hydrogen evolution over 0.5% Pt–$SrTiO_3$ is 797 μmol. Surprisingly, the amount of hydrogen evolution over 0.5% Cu–$SrTiO_3$ is 790 μmol, which is comparable

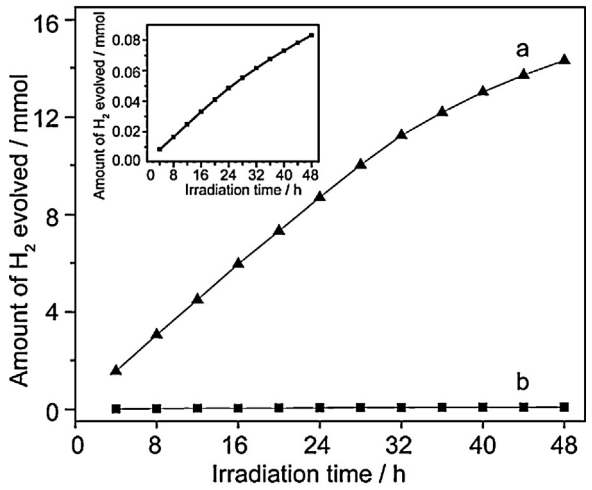

Fig. 4. Irradiation time dependence of amount of hydrogen evolution over (a) 0.5% Cu–$SrTiO_3$ and (b) pure $SrTiO_3$ at 45 °C (dosage of catalyst: 120 mg; methanol solution: 60 mL, 60 vol.%). The inset is magnified one of curve b.

Table 1
Photocatalytic hydrogen evolution over various photocatalysts (catalyst: 120 mg; methanol solution: 60 mL, 60 vol.%; temperature: 45 °C; irradiation time: 2 h).

Photocatalyst	Amount of hydrogen evolution (μmol)
pure $SrTiO_3$	4.13
0.5% Cu–$SrTiO_3$	790
0.5% Pt–$SrTiO_3$	797
1.0% Pt–$SrTiO_3$	857
1.5% Pt–$SrTiO_3$	968
2.0% Pt–$SrTiO_3$	1065
2.5% Pt–$SrTiO_3$	926
3.0% Pt–$SrTiO_3$	858

with that of 0.5% Pt–$SrTiO_3$. We thus believe that the metallic Cu could be an efficient alternative to Pt as a co-catalyst on $SrTiO_3$.

Based on the above results, a possible mechanism is displayed in Scheme 1 [24,29,30]. Under UV light irradiation, the electrons in the valence bands of $SrTiO_3$ nanoparticles are excited and transferred to their conduction bands. Then, Cu^{2+} ions are in situ reduced by the photogenerated electrons to form Cu particles on the surface of $SrTiO_3$ nanoparticles. When all Cu^{2+} ions are reduced, the photogenerated electrons begin to move to the Cu particles due to the Schottky barrier formed at the interface of Cu and $SrTiO_3$ [31]. Consequently, H^+ ions or water molecules are reduced into hydrogen by the photogenerated electrons on the surface of Cu particles, and the holes are consumed irreversibly through the reaction with methanol or water molecules. Herein, the loaded Cu particles act as charge transferring sites and/or active sites in the photocatalytic process. Thus, the recombination of the photogenerated electrons and holes is depressed, and the photocatalytic activity of $SrTiO_3$ is enhanced.

In order to further confirm the proposed mechanism, the DRS and the PL spectra of pure $SrTiO_3$ and 0.5% Cu–$SrTiO_3$ were investigated. As shown in Fig. 5A, the DRS of 0.5% Cu–$SrTiO_3$ is almost same as that of pure $SrTiO_3$, which all exhibit an absorption edge around 384 nm corresponding to band-gap of 3.22 eV calculated from the formula $E_g = 1240/\lambda$ [32]. The result indicates that loading of Cu does not change the band-gap of $SrTiO_3$ nanoparticles. It can be seen form Fig. 5B that the PL intensity of 0.5% Cu–$SrTiO_3$ is lower than that of pure $SrTiO_3$. This result demonstrates that there exists a transfer of photogenerated electrons from $SrTiO_3$ to Cu in 0.5% Cu–$SrTiO_3$ due to the Schottky barrier, which efficiently depresses the recombination of the photogenerated electrons and holes [33,34].

3.3. Effect of loading amount of Cu on the photocatalytic activity of $SrTiO_3$

The effect of loading amount of Cu on the photocatalytic hydrogen evolution over $SrTiO_3$ is shown in Fig. 6. It is observed that the amount of hydrogen evolution gradually increases from 158 μmol to 290 μmol with increasing the loading amount of Cu from 0.1 to 0.5 wt.% during the first 2 h irradiation. However, the amount of hydrogen evolution decreases dramatically when the loading

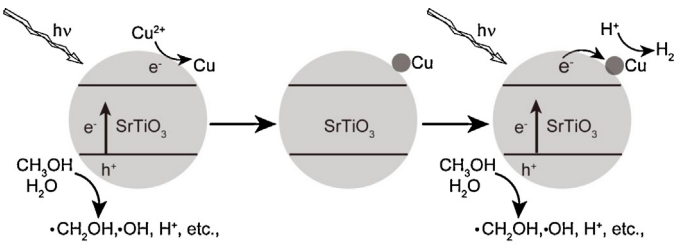

Scheme 1. Diagrams for the loading of Cu on the $SrTiO_3$ nanoparticles and the photocatalytic H_2 evolution over the Cu–$SrTiO_3$ nanoparticles under UV light irradiation.

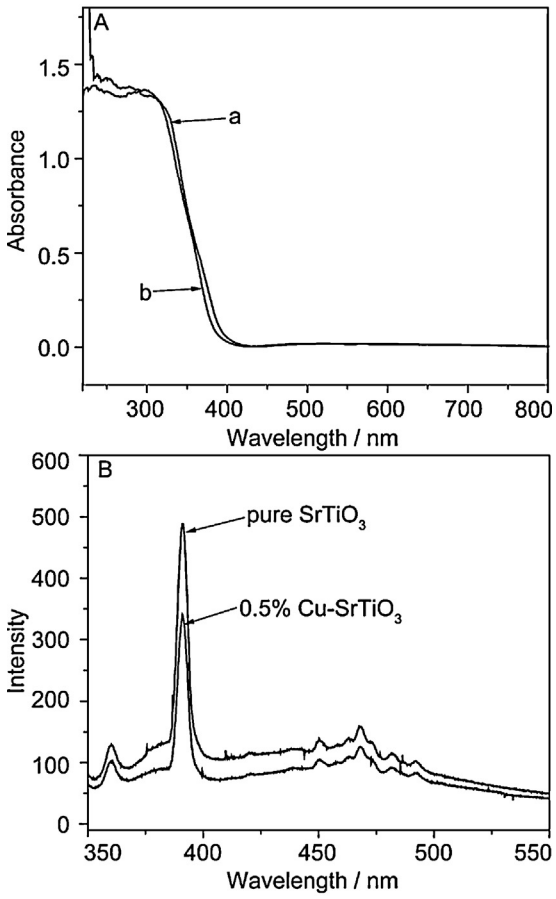

Fig. 5. A: DRS of (a) pure $SrTiO_3$ and (b) 0.5% Cu–$SrTiO_3$; B: PL spectra of pure $SrTiO_3$ and 0.5% Cu–$SrTiO_3$ (λ_{ex} = 339 nm).

amount of Cu further increases. One possible explanation is that the Cu particles on $SrTiO_3$ could act as the active sites of hydrogen evolution when the content of Cu is less than 0.5 wt.%. If the content of Cu is beyond 0.5 wt.%, the excess Cu would become the recombination sites of the photogenerated electrons and holes [35], leading to a decrease in the amount of hydrogen evolution. Thus, the optimum loading amount of Cu for $SrTiO_3$ is found to be 0.5 wt.%.

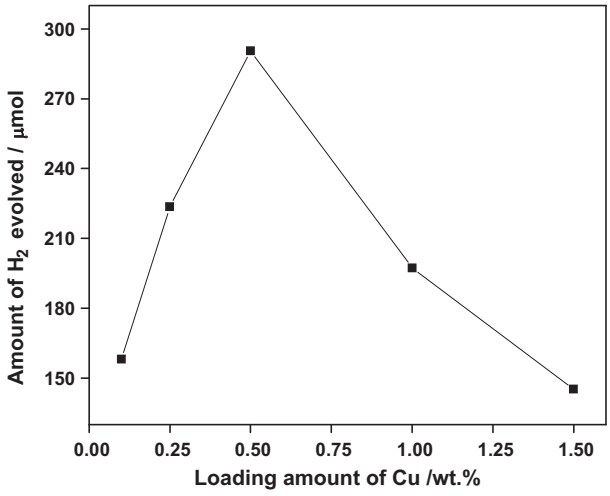

Fig. 6. Effect of loading amount of Cu on the photocatalytic hydrogen evolution of $SrTiO_3$ during the first 2 h irradiation (dosage of catalyst: 60 mg; methanol solution: 60 mL, 60 vol.%; reaction temperature: 25 °C).

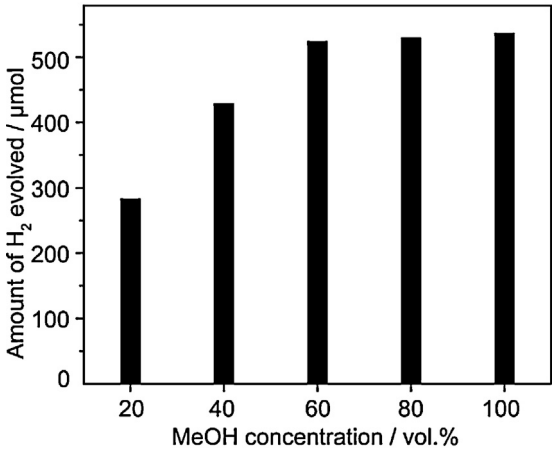

Fig. 7. Effect of methanol concentration on the photocatalytic hydrogen evolution of 0.5% Cu–$SrTiO_3$ during the first 2 h irradiation (dosage of catalyst: 60 mg; methanol volume: 60 mL; reaction temperature: 45 °C).

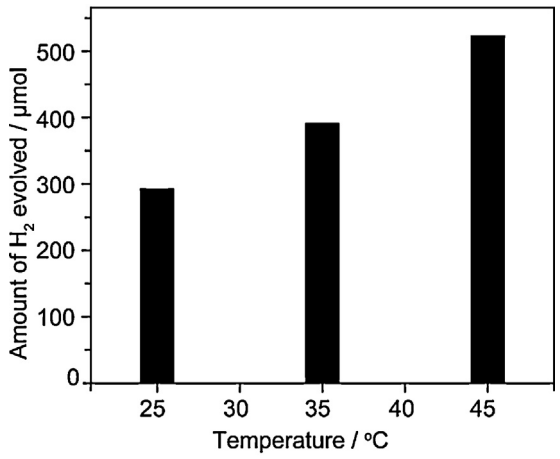

Fig. 8. Effect of reaction temperature on the photocatalytic hydrogen evolution of 0.5% Cu–$SrTiO_3$ (dosage of catalyst: 60 mg; methanol solution: 60 mL, 60 vol.%; irradiation time: 2 h).

3.4. Effect of methanol concentration on the photocatalytic activity of 0.5% Cu–$SrTiO_3$

Fig. 7 shows the effect of methanol concentration on the photocatalytic hydrogen evolution of 0.5% Cu–$SrTiO_3$. Obviously, the amount of hydrogen evolution enhances significantly with increasing the initial concentration of methanol from 20 vol.% to 60 vol.% during the first 2 h irradiation. However, the amount of hydrogen evolution is almost constant when the initial concentration of methanol is more than 60 vol.%. The possible reason is that the free methanol molecules in the solution are firstly adsorbed on the surface of the photocatalyst. Then, the adsorbed methanol molecules react with the photogenerated holes. When the concentration of methanol is low, the rate of adsorption is slower than that of photocatalytic reaction, and thus the amount of hydrogen evolution increases with increasing the concentration of methanol. If the concentration of methanol is higher than 60 vol.%, the rate of adsorption is relatively faster than that of photocatalytic reaction, which leads to almost constant amount of hydrogen evolution. Therefore, the optimum methanol concentration for the present photocatalytic system is 60 vol.%.

3.5. Effect of reaction temperature on the photocatalytic activity of 0.5% Cu–$SrTiO_3$

The effect of reaction temperature on the photocatalytic hydrogen evolution of 0.5% Cu–$SrTiO_3$ was studied. As shown in Fig. 8, the amount of hydrogen evolution over 0.5% Cu–$SrTiO_3$ enhances monotonously as the reaction temperature increases. The amount of hydrogen evolution at 45 °C (523 μmol) is about two times of that at 25 °C (292 μmol). This result demonstrates that the reaction temperature is a significant factor for the photocatalytic hydrogen evolution over Cu–$SrTiO_3$. Korzhak and co-workers have reported that the quantum yield of the photocatalytic hydrogen production of Cu-loaded TiO_2 nanoparticles increases with elevating temperature [23]. They ascribe the phenomenon to the thermal activation of the oxidized electron donor desorption and adsorption of donor. In addition, similar phenomena are reported by other researchers [11,36]. Therefore, it could be deduced that the influence of reaction temperature maybe originate from the faster adsorption of methanol molecules and the faster desorption of the oxidation products of methanol and hydrogen evolved. Because more than 45 °C of the reaction temperature will lead to rapid evaporating of water, the optimum reaction temperature is selected to be 45 °C.

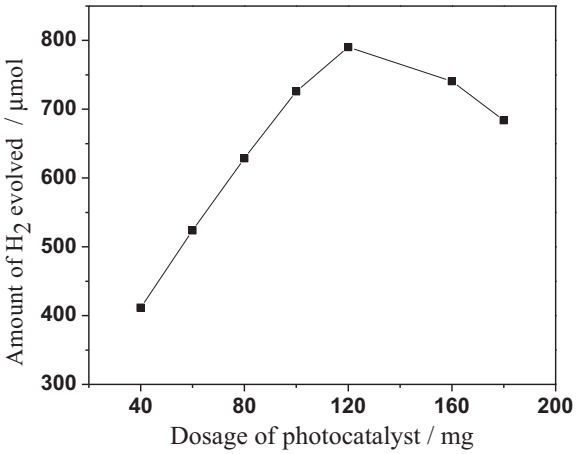

Fig. 9. Effect of dosage of photocatalyst on the photocatalytic activity of 0.5% Cu–$SrTiO_3$ at 45 °C (methanol solution: 60 mL, 60 vol.%; irradiation time: 2 h).

3.6. Effect of dosage of catalyst on the photocatalytic activity of 0.5% Cu–$SrTiO_3$

Fig. 9 shows the effect of dosage of photocatalyst on the photocatalytic hydrogen evolution of 0.5% Cu–$SrTiO_3$. Obviously, the amount of hydrogen evolution increases significantly from 411 μmol to 790 μmol when the dosage of 0.5% Cu–$SrTiO_3$ increases from 40 mg to 120 mg. Whereas, the amount of hydrogen evolution decreases gradually from 790 μmol to 683 μmol when the dosage of 0.5% Cu–$SrTiO_3$ is more than 120 mg. One possible explanation is that the available active sites increase with increasing the dosage of 0.5% Cu–$SrTiO_3$. If the dosage of 0.5% Cu–$SrTiO_3$ is excess, the UV light through the reaction system is greatly scattered by the suspended photocatalysts, and the effective light absorption of the system will reduce. Consequently, the amount of hydrogen evolution decreases [30]. Therefore, the optimum dosage of the photocatalyst is selected to be 120 mg.

4. Conclusions

In summary, the metallic Cu can be homogeneously loaded on the surface of $SrTiO_3$ nanoparticles using a simple in situ photodeposition method. The results show that the Cu–$SrTiO_3$ is a highly active, cheap and stable photocatalyst for the hydrogen evolution

from the methanol aqueous solution under UV light irradiation. The metallic Cu as a co-catalyst is a potential alternative to noble metals.

Acknowledgements

This work was financially supported by the Key Project of the National Natural Science Foundation of China (No. 20933007) and the National High Technology Research and Development Program of China (No. 2009AA05Z101).

References

[1] B.S. Huang, F.Y. Chang, M.Y. Wey, International Journal of Hydrogen Energy 35 (2010) 7699–7705.
[2] M. Ni, M.K.H. Leung, D.Y.C. Leung, K. Sumathy, Renewable and Sustainable Energy Reviews 11 (2007) 401–425.
[3] B. Wang, C.S. Li, D. Hirabayashi, K. Suzuki, International Journal of Hydrogen Energy 35 (2010) 3306–3312.
[4] Y. Guo, S.Z. Wang, D.H. Xu, Y.M. Gong, H.H. Ma, X.Y. Tang, Renewable and Sustainable Energy Reviews 14 (2010) 334–343.
[5] X.B. Chen, S.H. Shen, L.J. Guo, S.S. Mao, Chemical Reviews 110 (2010) 6503–6570.
[6] A. Kudo, Pure and Applied Chemistry 79 (2007) 1917–1927.
[7] X.B. Chen, S.S. Mao, Chemical Reviews 107 (2007) 2891–2959.
[8] A. Kudo, Y. Miseki, Chemical Society Reviews 38 (2009) 253–278.
[9] A.Z. Jia, Z.Q. Su, L.L. Lou, S.X. Liu, Solid State Sciences 12 (2010) 1140–1145.
[10] X.G. Guo, X.S. Chen, Y.L. Sun, L.Z. Sun, X.H. Zhou, W. Lu, Physics Letters A 317 (2003) 501–506.
[11] T. Puangpetch, T. Sreethawong, S. Yoshikaw, S. Chavadej, Journal of Molecular Catalysis A: Chemical 312 (2009) 97–106.
[12] H.B. Yi, T.Y. Peng, D.N. Ke, D. Ke, L. Zan, C.H. Yan, International Journal of Hydrogen Energy 33 (2008) 672–678.
[13] S. Ikeda, K. Hirao, S. Ishino, M. Matsumura, B. Ohtani, Catalysis Today 117 (2006) 343–349.
[14] C.C. Lo, C.W. Huang, C.H. Liao, J.C.S. Wu, International Journal of Hydrogen Energy 35 (2010) 1523–1529.
[15] Y.J. Hui, Z.Y. Rong, T.Y. Gen, Z.S. Qin, Journal of Alloys and Compounds 472 (2009) 429–433.
[16] K. Domen, S. Naito, T. Onishi, K. Tamaru, Journal of Physical Chemistry 86 (1982) 3657–3661.
[17] K. Domen, A. Kudo, T. Onishi, Journal of Catalysis 102 (1986) 92–98.
[18] K. Domen, A. Kudo, T. Onishi, Journal of Physical Chemistry 90 (1986) 292–295.
[19] R. Niishiro, H. Kato, A. Kudo, Physical Chemistry Chemical Physics 7 (2005) 2241–2245.
[20] Y. Qin, G.Y. Wang, Y.J. Wang, Catalysis Communications 8 (2007) 926–930.
[21] Y. Liu, L. Xie, Y. Li, R. Yang, J.L. Qu, Y.Q. Li, X.Q. Li, Journal of Power Sources 183 (2008) 701–707.
[22] T. Puangpetch, T. Sreethawong, S. Chavadej, International Journal of Hydrogen Energy 35 (2010) 6531–6540.
[23] A.V. Korzhak, N.I. Ermokhina, A.L. Stroyuk, V.K. Bukhtiyarov, A.E. Raevskaya, V.I. Litvin, S.Y. Kuchumiy, V.G. Ilyin, P.A. Manorrik, Journal of Photochemistry and Photobiology A 198 (2008) 126–134.
[24] H.J. Choi, M. Kang, International Journal of Hydrogen Energy 32 (2007) 3841–3848.
[25] S.P. Xu, J.W. Ng, X.W. Zhang, H.W. Bai, D.D. Sun, International Journal of Hydrogen Energy 35 (2010) 5254–5261.
[26] T. Sreethawong, S. Yoshikawa, Catalysis Communications 6 (2005) 661–668.
[27] N.L. Wu, M.S. Lee, International Journal of Hydrogen Energy 29 (2004) 1601–1605.
[28] L. Chen, S.C. Zhang, L.Q. Wang, D.F. Xue, S. Yin, Journal of Crystal Growth 311 (2009) 735–737.
[29] X.J. Zheng, L.F. Wei, Z.H. Zhang, Q.J. Jiang, Y.J. Wei, B. Xie, M.B. Wei, International Journal of Hydrogen Energy 34 (2009) 9033–9041.
[30] K. Lalitha, J.K. Reddy, V.P.M. Sharma, V.D. Kumari, M. Subrahmanyam, International Journal of Hydrogen Energy 35 (2010) 3991–4001.
[31] A.L. Linsebigler, G.Q. Lu, J.T. Yates Jr., Chemical Reviews 95 (1995) 735–758.
[32] S. Onsuratoom, S. Chavadej, T. Sreethawong, International Journal of Hydrogen Energy 36 (2011) 5246–5261.
[33] I.J. Lee, T. Jung, J.G. Kim, S.H. Ro, C.S. Kim, Y.J. Lee, Y.M. Kim, J.Y. Lee, M.S. Kang, Journal of Industrial and Engineering Chemistry 14 (2008) 869–873.
[34] T. Kiyonaga, M. Fujii, T. Akita, H. Kobayashi, H. Tada, Physical Chemistry Chemical Physics 10 (2008) 6553–6561.
[35] T. Ishii, H. Kato, A. Kudo, Journal of Photochemistry and Photobiology A 163 (2004) 181–186.
[36] V.M. Daskalaki, D.I. Kondarides, Catalysis Today 144 (2009) 75–80.